Journal of Nuclear and Particle Physics 2014, 4(6): 155-163
DOI: 10.5923/j.jnpp.20140406.01

Microscopic Study of Nuclear Structure for Some Zr-isotopes Using Skyrme-Hartree-Fock-Method

Ali A. Alzubadi[1], Z. A. Dakhil[1], Sheimaa T. Aluboodi[2,*]

[1]Department of physics, College of Science, University of Baghdad, Iraq
[2]Dijlah College University, Baghdad, Iraq

Abstract In the present research the ground state nuclear structure of Zr-isotopes has been investigated within the framework of Skyrme-Hartree-Fock using the Skyrme parameterizations; SkM*, S1, S3, SkM, and SkX. The charge, proton, neutron and mass densities together with their associated root mean square radii, neutron skin thicknesses, nuclear binding energies, and charge form factors have been calculated. The effects of Skyrme parameterizations on the calculated values of the static nuclear properties of the selected isotopes have been disclosed in appropriate figures. It can be deduced from this research that it is the SkX parameterization which achieves the best agreement with the experimental data as compared with the other parameterizations. Comparison between the theoretical and experimental results of charge form factors has likewise been performed.

Keywords Skyrme-Hartree-fock method, Zr-isotopes

1. Introduction

The nuclear density distribution is one of the basic quantities for describing the nuclear structure. It can give detailed information on the internal structure of nuclei since they are directly related to the wave functions of the protons and neutrons which are important keys to many calculations in nuclear physics. Also the nuclear charge radii represent the most useful observables for analyzing the nuclear structure. These observables provide information about the nuclear shape which can be determined from the form factors.

In the present research, the ground state properties of Zr-isotopes will be investigated in details using Skyrme-Hartree-Fock (SHF) method which has been used successfully to describe the ground state properties of stable nuclei [1-3]. In particular, we will investigate the static nuclear properties namely, the charge, proton, neutron and mass densities together with their associated root mean square (rms) radii, neutron skin thicknesses, total nuclear binding energies, and charge form factors. The calculated results will then be compared with the available experimental data for the said isotopes.

2. Theory and Methodology

The Skyrme effective interaction was first proposed in the work of Vautherin and Brink [4]. It was introduced in the Hartree-Fock (HF) calculations of nuclei [5]. Until now, the SHF method has been successfully and widely used for studying the nuclear structure [2]. The Skyrme force is an effective interaction with a two-body and a three-body parts [6]. The two body term is written as a short range expansion in the form [7]:

$$\begin{aligned} V_{Skyrme} &= t_0\left(1+x_0\hat{P}_\sigma\right)\delta(\vec{r}) \\ &+\frac{1}{2}t_1\left(1+x_1\hat{P}_\sigma\right)\left[\delta(\vec{r})\vec{k}^2+\vec{k}'^2\delta(\vec{r})\right] \\ &+t_2\left(1+x_2\hat{P}_\sigma\right)\vec{k}'.\delta(\vec{r})\vec{k} \\ &+\frac{1}{6}t_3\left(1+x_3\hat{P}_\sigma\right)\rho^\alpha\left(\vec{R}\right)\delta(\vec{r}) \\ &+it_4\vec{k}'.\delta(\vec{r})\left(\vec{\sigma}_i+\vec{\sigma}_j\right)\vec{k}\,, \end{aligned} \quad (1)$$

where the $\hat{k}=\frac{1}{2i}(\nabla_1-\nabla_2)$ and $\hat{k}'=-\frac{1}{2i}(\nabla_1'-\nabla_2')$ operators are the relative (momentum) wave vectors of two nucleons. $\hat{k}$ acts to the right and $\hat{k}'$ to the left. $\delta(\vec{r})$ is the delta function. $\hat{P}_\sigma$ is the space exchange operator, $\vec{\sigma}$ the vector of Pauli spin matrices and the $t_0,t_1,t_2,t_3,t_4,x_0,x_1,x_2,x_3$ and α are the Skyrme force parameters describing the strengths of the different interaction terms [8]. The values of these parameters for different parameterizations are listed in Table.1.

The Hamiltonian is written in terms of kinetic energy and two-body nucleon-nucleon interaction [12]:

$$\hat{H}=\sum_{i=1}^{A}\frac{\hat{p}_i^{\,2}}{2m_i}+\frac{1}{2}\sum_{i\neq j}^{A}V(\boldsymbol{r_i},\boldsymbol{r_j}). \quad (2)$$

* Corresponding author:
sheimaathiab@yahoo.com (Sheimaa T. Aluboodi)
Published online at http://journal.sapub.org/jnpp

In this representation of the Hamiltonian the nucleon-nucleon interaction characterizes the many-particle Schrodinger equation. In the SHF approach the total binding energy of the system is given by the sum of the kinetic and Coulomb energies as well as the Skyrme energy functional that models the effective interaction between nucleons [13]

$$E = E_{Coul} + E_{Kin} + \int \varepsilon_{Sky}\, dr + E_{pair} + E_{Cm}\,. \quad (3)$$

By substituting the Skyrme interaction terms into the full energy expression, the form of the density function $\hat{H}(r)$ can be written as [14].

$$\langle \Phi|\hat{H}|\Phi\rangle = -\frac{\hbar^2}{2m}\sum_{i=1}^{A}\int dr_1\, \emptyset_i^*(r_1)\nabla_i^2\emptyset_i(r_1)$$

$$+\frac{1}{2}\sum_{ij\,\sigma_1\sigma_2 q_1 q_2}\iint d^3r_1\, d^3r_2 \phi_i^*(r_1,\sigma_1,q_1)\phi_j^*(r_2,\sigma_2,q_2)$$

$$V(r_1,r_2)\left(1-\hat{P}_M\hat{P}_\sigma\hat{P}_q\right)\phi_i(r_1,\sigma_1,q_1)\phi_j(r_2,\sigma_2,q_2). \quad (4)$$

The ground-state charge density $\rho(r)_{ch}$, gives the most direct physical insight into the distribution of protons inside the nucleus. The densities in spherical representation are given by [15]:

$$\rho_q(r) = \sum_{n_\beta j_\beta l_\beta} \omega_\beta \frac{2j_\beta+1}{4\pi}\left(\frac{R_\beta}{r}\right)^2, \quad (5)$$

where q represents the neutron, proton and charge, ω_β is the occupation probability of the state β and j_β is the current density that vanishes for the ground states. The charge probability density [16].

$$P(r)_{ch} = 4\pi r^2 \rho(r)_{ch} \quad (6)$$

$P(r)_{ch}$ represents the probability to find Z protons at a given radius r from the center of the nucleus. The rms radii of neutron, proton, charge and mass distributions can be evaluated from these densities as [17]:

$$r_q = \langle r_q{}^2\rangle^{1/2} = \left[\frac{\int r^2 \rho_q(r)\mathrm{d}r}{\int \rho_q(r)\mathrm{d}r}\right]^{1/2} \quad (7)$$

where q = neutron, proton or charge. A quantity of both theoretical and experimental interest, the neutron skin thickness t, can then be defined as the difference between the neutron rms radius and the proton rms radius [18]:

$$t = r_n - r_p = \langle r_n{}^2\rangle^{1/2} - \langle r_p{}^2\rangle^{1/2}. \quad (8)$$

The concept of form factor is associated with the charge density and its properties. Elastic electron scattering from nuclei constitutes an important source of experimental data on charge densities which are measurable and with which the models for nuclear ground states can be tested. Electron scattering evolved from the early determinations of rms charge radii to the present much more precise measurements that have led to almost model- independent determinations of the charge density distributions of many nuclei. In these density distributions one can observe oscillations in the interior density which oscillations represent quantum "waves" in the nucleus [19]. Denoting by $F(q)$ the ratio of the electron scattering cross section to the Rutherford cross section (scattering from a point) as a function of momentum transfer, q, one will find that this ratio expresses the plane-wave Fourier transform of the charge density as follows [17]:

$$F(q) = \frac{1}{z}\int \rho(r)_{ch}\, e^{i\vec{q}.\vec{r}}\, d\tau = \frac{4\pi}{z}\int \rho(r)_{ch}\, j_0(qr) r^2 dr, \quad (9)$$

where the spherical Bessel function is:

$$j_0(qr) = \frac{\sin qr}{qr} \quad (10)$$

The normalization in Eq. (9) is chosen to give $F(q=0)$ =1. For light nuclei the electron energy distortion is small, and the cross section is closely proportional to the form factor $|F(q)|^2$ which has minima corresponding to the zeros of the function $F(q)$. For heavy nuclei the electron energy distortion is larger and the minima in the cross sections disappear. From an analysis of the electron scattering cross section the ratio $F(q)$ can be extracted with good precision over the range of momentum transfers measured. Consequently, from the measured form factors $|F(q)|^2$ the charge density can be obtained with the inverse of Eq. (9) [19]:

$$\int \rho(r)_{ch} dr = \frac{z}{2\pi^2}\int F(q)\, j_0(qr) q^2 dq \quad (11)$$

Since the form factors data are only determined up to some q_{max} the resulting charge density has some "error band" which depends on the assumptions made about $F(q)$ for $q > q_{max}$.

Table 1. The Skyrme parameterizations that have been used in the present research

Force	SkM* [9]	S1[5]	S3[5]	SkM [10]	SkX [11]
t_0 (MeV ·fm^3)	−2645.0	−1057.3	−1128.75	−2645.0	-1445.3
t_1 (MeV ·fm^5)	410	235.9	395	385	246.9
t_2 (MeV ·fm^5)	−135.0	−100.0	−95.0	−120.0	-131.8
t_3 (MeV ·fm^3)	15595	14463.5	14000	15595	12103.9
t_4 (MeV ·fm^5)	130	0	120	130	
x_0	0.09	0.56	0.45	0.09	0.34
x_1	0	0	0	0	0.58
x_2	0	0	0	0	0.127
x_3	0	1	1	0	0.03
α	1/6	1	1	1/6	0.5

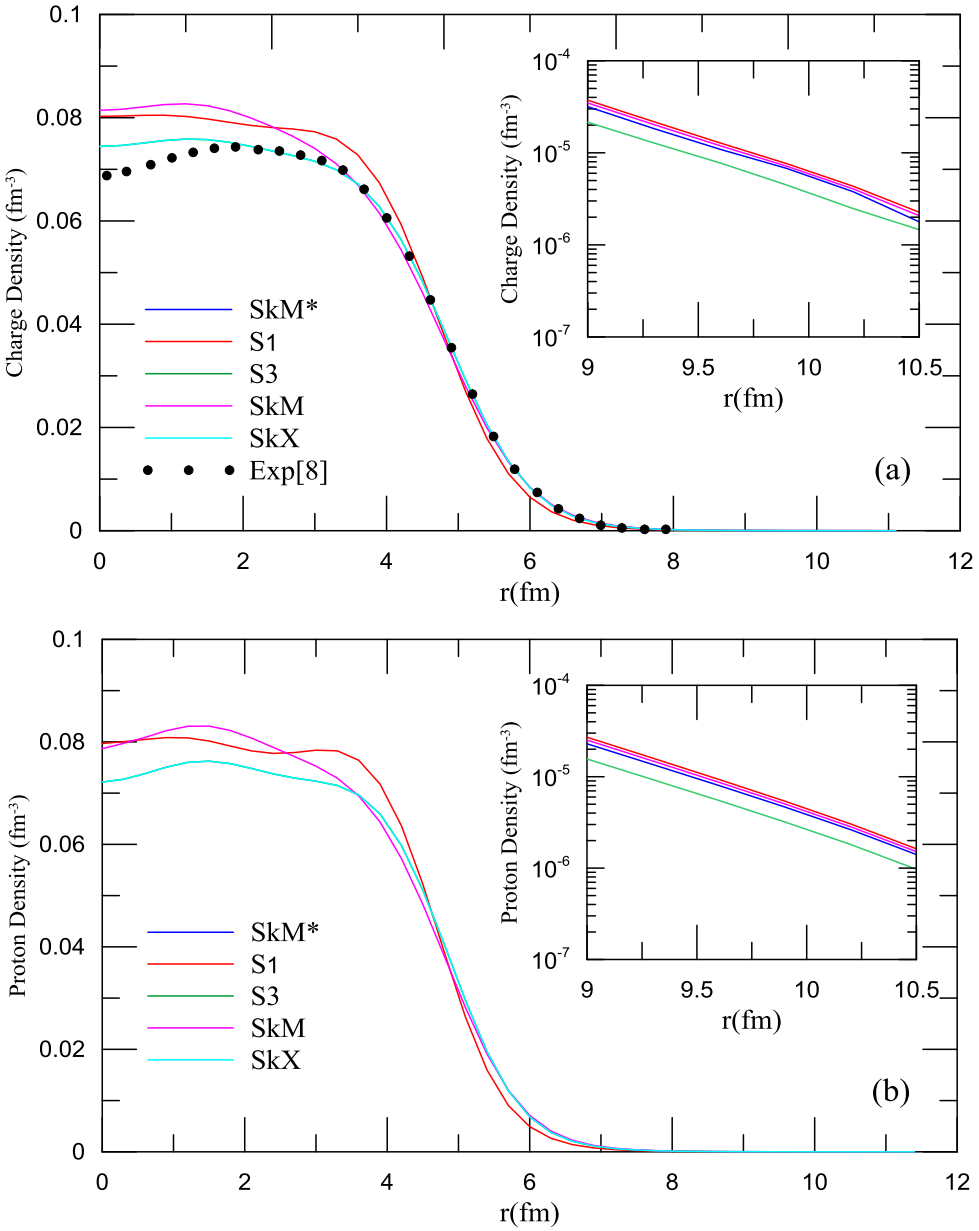

Figure (1). Density profiles of ^{90}Zr-isotopes as functions of radii calculated using different Skyrme parameterizations; (a) charge (b) protons

3. Results and Discussion

We will employ the experimental data on charge density available for the isotope ^{90}Zr taken from Ref. [8]. The density distribution of ^{90}Zr isotope has been calculated using five selected parameterizations and shown in Figs.(1) and (2). Inspection of the charge density profiles reveal that the best agreement between the calculated and experimental data is obtained using the SkX- parameterizations shown in Fig.(1a).

Consequently we applied the SkX-parameterization to all the other Zr-isotopes. The values thus obtained for the charge density of these isotopes at the center, r = 0, decrease with the increasing number of neutrons approximately from (0.082371) fm^{-3} for ^{78}Zr to (0.067104) fm^{-3} for ^{102}Zr as shown in Fig. (3a) And the proton density decreases with the increasing neutron number approximately from (0.0827) fm^{-3} for ^{78}Zr to (0.067764) fm^{-3} for ^{102}Zr as shown in Fig. (3b).

In general point of view, it can be noted that with increasing number of neutrons in the succeeding isotopes of the same element the neutron density increases whereas the proton density decreases accordingly. This behavior applies to the range range r >1.8 fm, but is violated for the range 0 ~ 1.8 fm, as can be seen clearly in Fig. (4a). The mass density is also governed by the same behavior which applies to the range r > 3.2 fm but is violated for the range r ≤ 3.2 fm as in Fig. (4b). In this range the abnormality (randomness) in the behavior of the isotopes (i.e. oscillations in density values) is due to the diffusion of the nuclear matter in the vicinity of the center of the nucleus. This abnormal behavior results from the stretching of the density distribution as the isotopes

increase progressively in mass number. Consequently, the applied Skyrme parameterization fails to give an exact description in the said region.

For more illustration the calculated charge density distributions for Si-isotopes are displayed as a surface in Fig. (5). These distributions are plotted against the nuclear masses which are decreasing (in viewing into the page). These variations of charge densities are best portrayed in block form.

Although experimental data on charge probability density may not be available, it can, however, be easily calculated from the experimental data already available on nuclear charge density that was employed in calculating the probability densities. The calculated and experimental charge probability densities of the ^{90}Zr are in good agreement as shown clearly in Fig. (6).

The rms charge radius is a fundamental property of the atomic nucleus. The rms radii of charge distributions can be evaluated from the charge densities according to Eq. (7). As can be seen from Table 2 below the calculations by the SHF-method of the nuclear charge rms radii of the Zr isotopes reveal a good conformity among the values in each row separately i.e., for each isotope, and in all the rows combined. All the values based on the different parameter sets considered in the table have more or less the same value. The rms charge radii for ^{78} Zr and ^{102} Zr decrease only slightly from (4.2656) and (4.3894) by SkM* to (4.1443) and (4.3170) by S1 as shown below.

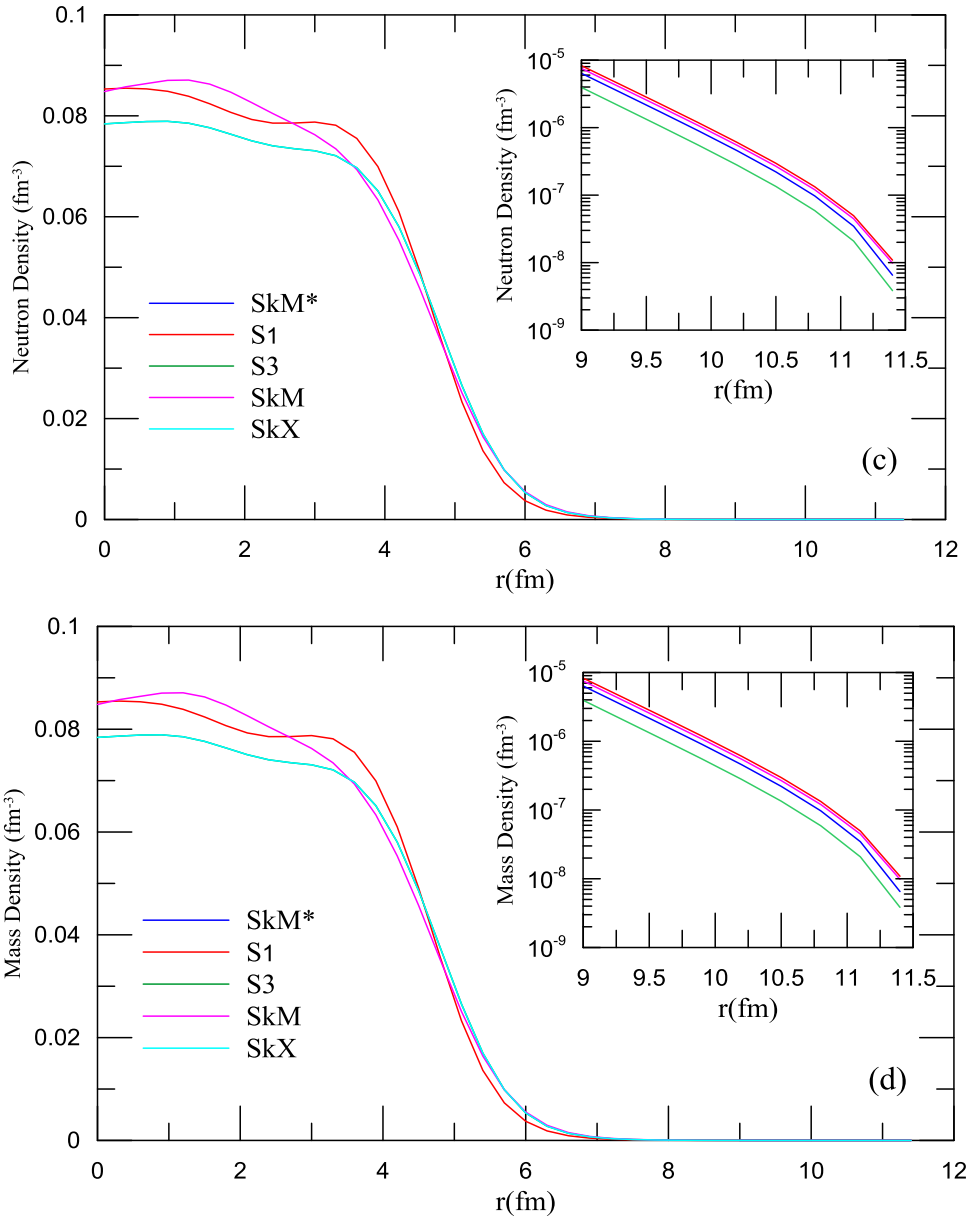

Figure (2). Density profiles of ^{90}Zr-isotopes as functions of radii calculated using different Skyrme parameterizations; (c) neutrons (d) mass

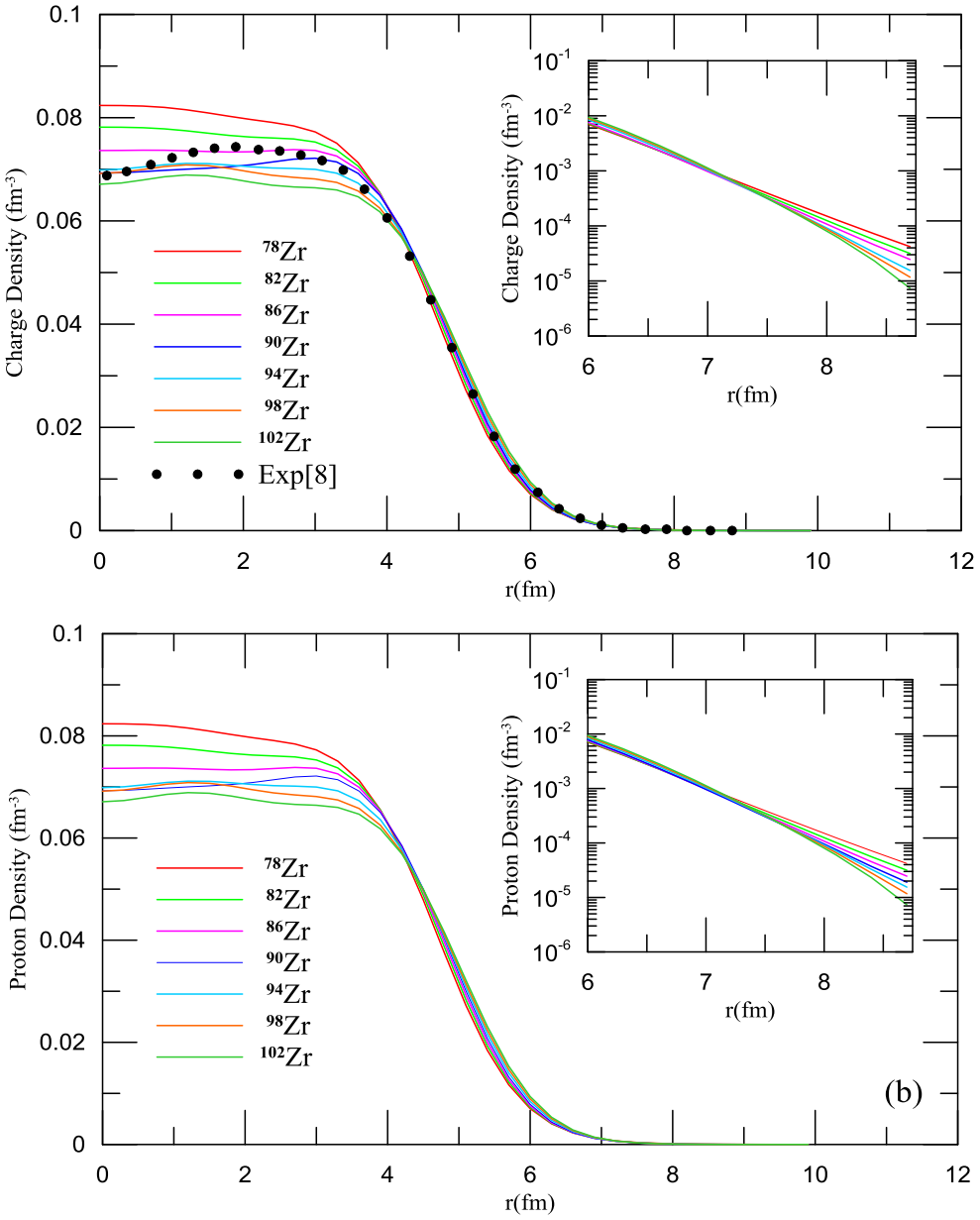

Figure (3). Density profiles of Zr-isotopes as functions of radii calculated using SkX parameterizations; (a) charge (b) protons

Table 2. Calculation of nuclear charge rms radii compared with experimental data from Ref. [17]

Nucleus	SkM*	S1	S3	SkM	SkX	Exp(rms)
^{78}Zr	4.2656	4.1443	4.2660	4.2455	4.1660	……..
^{82}Zr	4.2765	4.1660	4.2871	4.2566	4.1877	……..
^{86}Zr	4.2821	4.1861	4.3042	4.2626	4.2097	……..
^{90}Zr	4.2907	4.2074	4.323	4.2713	4.2322	4.2696
^{94}Zr	4.3179	4.242	4.3612	4.2991	4.2587	4.3312
^{98}Zr	4.3487	4.2787	4.3995	4.3306	4.2848	4.4185
^{102}Zr	4.3894	4.3170	4.4382	4.3723	4.3119	4.5690

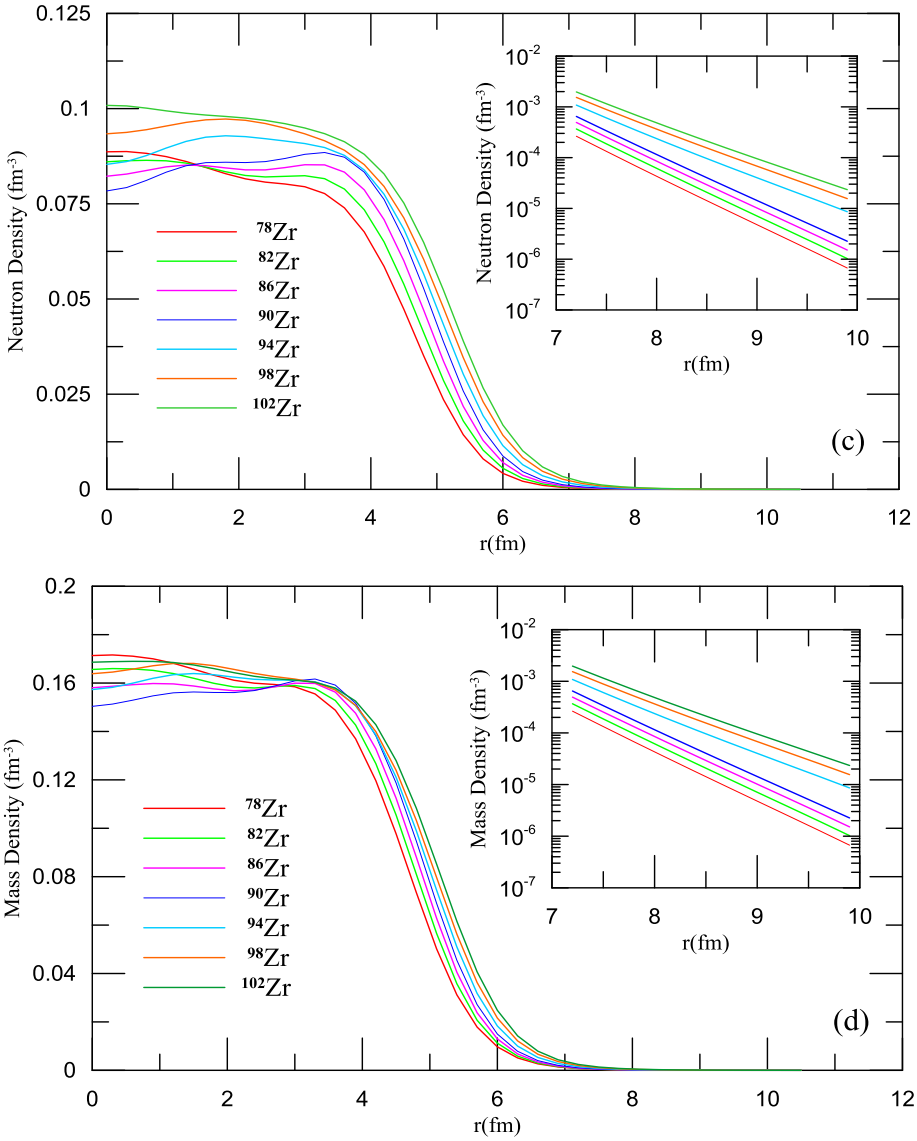

Figure (4). Density profiles of Zr- isotopes as functions of radii calculated using SkX parameterization; (c) neutron (d) mass

As to the nuclear binding energies, Fig. (7) shows a comparison between the experimental and theoretical values for the Zr-isotopes. The Skyrme parameterizations SkM*, S1, S3, SkM, and SkX are used in the calculations. Except for some slight deviations in the S1- curve all the other curves generally show the same behavior wherein the binding energy increases with increasing mass number.

Table 3. Calculated values of Binding energy compared with experimental data from Ref. [20]

Nucleus	SkM*	S1	S3	SkM	SkX	Exp(B.E)
^{78}Zr	626.69	645.48	626.21	636.73	663.47	……..
^{82}Zr	681.00	702.16	680.70	691.60	720.84	694.745
^{86}Zr	729.38	754.29	729.12	740.73	775.34	740.6492
^{90}Zr	773.49	801.14	772.98	785.53	824.62	783.891
^{94}Zr	803.84	825.92	798.56	815.21	852.92	814.6792
^{98}Zr	829.29	846.55	821.23	840.03	876.01	831.9024
^{102}Zr	851.02	865.45	842.94	861.21	895.57	863.7258

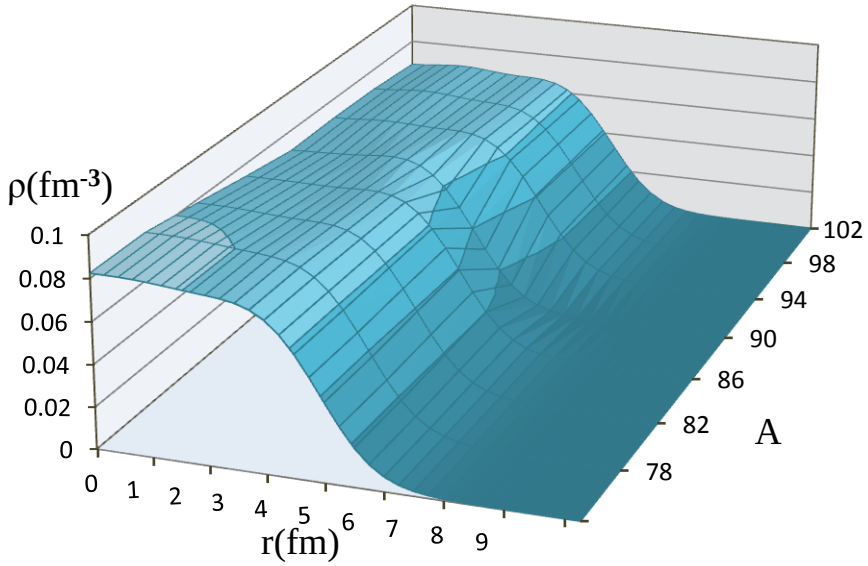

Figure (5). Charge density variation with mass number A from SkX parameterization for different Zr-isotopes

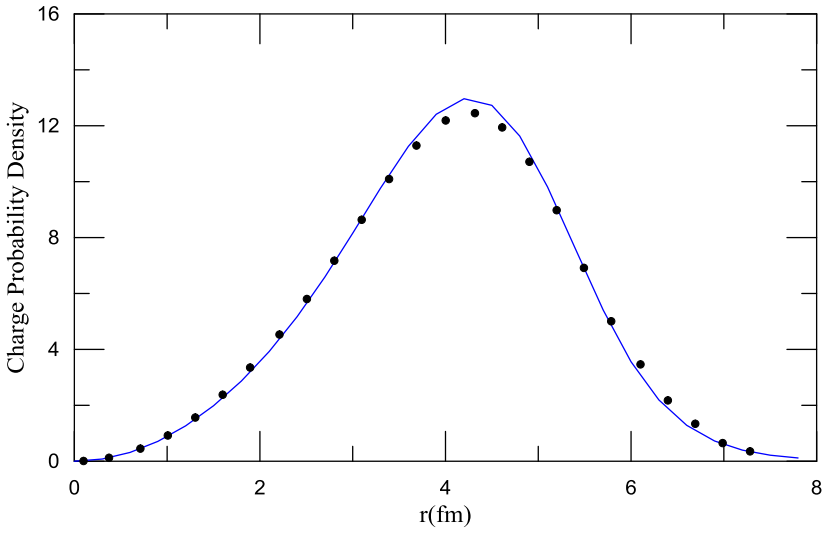

Figure (6). Charge probability density distributions for ^{90}Zr isotope using SkX parameterization

Table 4. The skin thickness of Zr isotopes calculated using different Skyrme parameterizations

Isotopes	SkM*	S1	S3	SkM	SkX
^{78}Zr	-0.117	-0.093	-0.102	-0.116	-0.101
^{82}Zr	-0.047	-0.04	-0.044	-0.045	-0.04
^{86}Zr	0.014	0.006	0.009	0.016	0.012
^{90}Zr	0.066	0.045	0.054	0.068	0.054
^{94}Zr	0.137	0.098	0.112	0.139	0.113
^{98}Zr	0.198	0.141	0.158	0.201	0.164
^{102}Zr	0.253	0.177	0.197	0.256	0.208

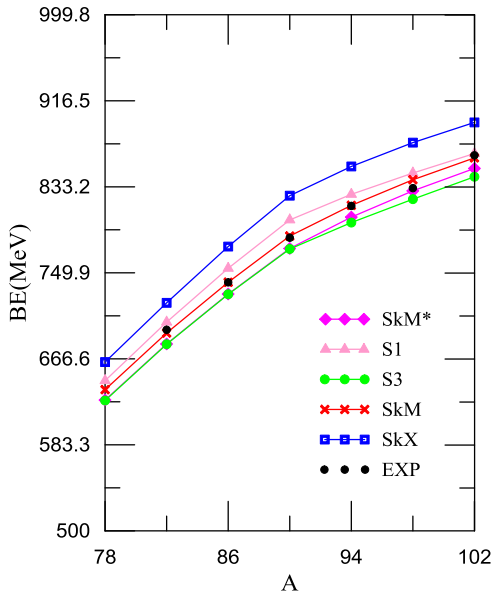

Figure (7). The binding energy of Zr-isotopes calculated using different Skyrme parameterizations

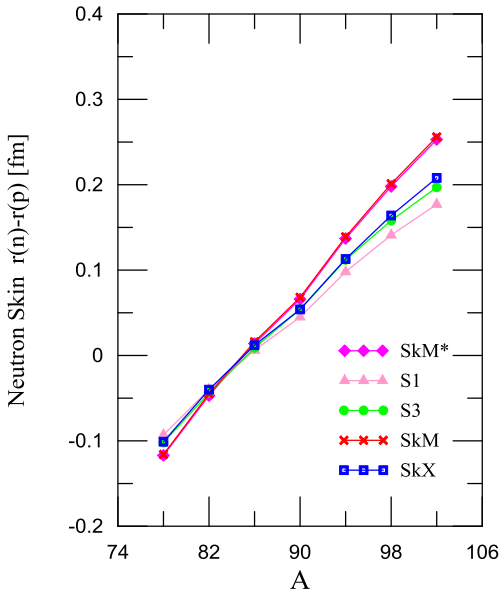

Figure (8). The neutron skin thickness of Zr-isotopes calculated using different Skyrme parameterizations

The SkM* based binding energies have the highest values for all the isotopes of each of the four element whereas the S3 values are the lowest. The SkM binding energy values turn out to be in full agreement with the experimental data as can be clearly seen in Table 3. For this reason we have selected the SkM parameterization as a basis for calculating the form factors of the selected nuclides.

The skin thickness of a nucleus is defined as the distance over which the charge density drops from 90% to 10% of its maximal value. The thickness is almost the same for all heavy nuclei and is given by: $t = 2a \ln 9 \sim 2.40$ fm [21]. The growth of the neutron skin with increasing neutron number was calculated for several isotopes from nuclear and charge-size data [22]. The neutron skin thickness of Zr isotopes increases with increasing mass number along all the curves plotted by the different Skyrme parameterizations as shown in Fig. (8). In Table 4 the quantity t for some of the isotopes have negative values because the force tend to spread the protons a little and becomes increase in positive with increasing the neutron excess.

From the charge densities shown in Fig. (2a), the scattering amplitude form factors $|F(q)|^2$ were calculated for the Zr-isotopes and shown in Fig. (9). In this figure the hollow circles stand for the experimental data [16] given over the range of momentum transfers measured experimentally. The said experimental data were then compared with the theoretical values of the form factors calculated using the SkX parameterization. It is found that there is a fine agreement in the range of momentum transfer ≤ 2.4 fm^{-1}. For greater values, the theoretical values deviate and become less than the experimental data.

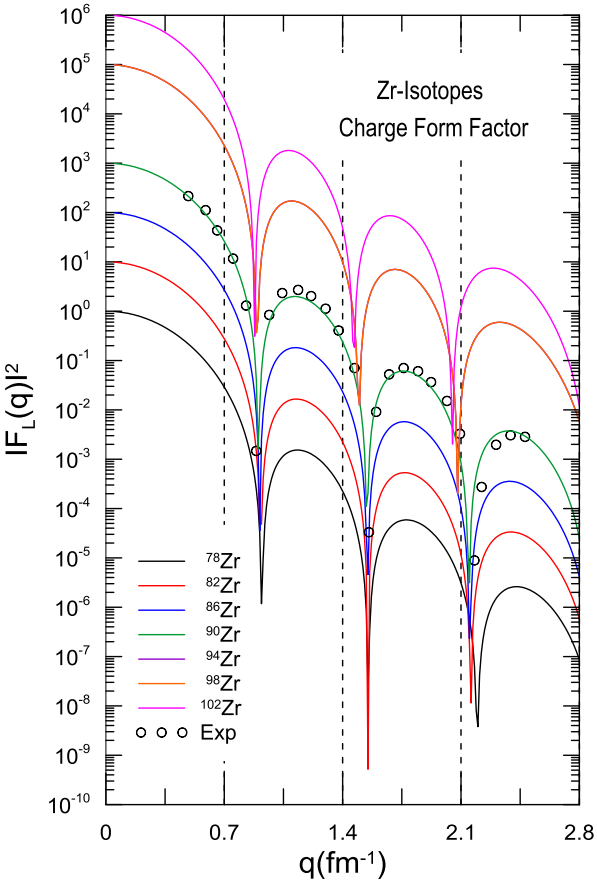

Figure (9). Charge form factors versus momentum transfer q(fm^{-1}) for ^{78}Zr, ^{82}Zr (×10), ^{86}Zr (×10^2), ^{90}Zr (×10^3), ^{94}Zr (×10^4), ^{98}Zr (×10^5), and ^{102}Zr (×10^6) isotopes. The experimental data are taken from Ref. [16]

This deviation is ascribed to two factors. First, the Skyrme interaction approximation undergoes a low-momentum expansion, and the density fluctuation resulting from this approximation is expected to break down at some point. Second, mesonic-exchange corrections to the charge form factor become increasingly important at higher momentum transfers [18].

4. Conclusions

The above calculations show that the best agreement between the theoretical values and experimental data is better achieved for nuclear charge density by the SkX parameterization than by the others. However in the vicinity of the nucleus center (on the range $r < 2$ fm) the isotopes behave randomly with oscillating density values due to the diffusion (stretching) of the nuclear matter, which makes Skyrme parameterizations fail to give an exact description in the said region. As to the binding energy the best agreement between calculations and experimental data is achieved by SkM parameterization. The comparison between experiment and theory in terms of form factors have been discussed, where the data are taken over the range of momentum measured, and in terms of the charge densities. Rapid oscillations may occur in the experimental densities. Comparison with experiment will provide a test for the mean-field models.

REFERENCES

[1] J.W. Negele and D. Vautherin, Phys. Rev. C5 (1972)1472.

[2] J. Friedrich and P.-G. Rienhard, Phys. Rev. C33 (1986) 335.

[3] J. Dobaczewski, I. Hamamoto, W. Nazarewicz and J.A. Sheikh, Phys. Rev. Lett. 72(1994)981.

[4] T. H. Skyrme, Phil. Mag. 1 (1956) 1043; Nucl. Phys. 9 (1959) 615.

[5] D. Vautherin and D. M. Brink, Phys. Rev. C5 (1972) 626.

[6] Skyrme, T. The Effective Nuclear Potential. Nuclear Physics, 9 (1959) 615.

[7] W. Greiner and j. Maruhn, "Nuclear Models" 2nd Ed., Springer-verlge Berlin (1996).

[8] L.G. Qiang, J. Phys. G 17 (1991) 134.

[9] J. Bartel, P. Quentin, M. Brack, C. Guet and M.B. Hakansson, Nucl. Phys. A386 (1982) 79.

[10] L.X. Ge, Y.Z. Zhuo, and W. Norenberg, Nucl. Phys. A459 (1986) 77.

[11] B.A. Brown, Phys. Rev. C58 (1998) 220.

[12] E. Suckling, PhD thesis, University of Surrey (2011).

[13] M. Bender, P. H. Heenen and P. G. Reinhard, Rev. Mod. Phys. 75 (2003) 121.

[14] E. Suckling, MsC thesis, University of Surrey (2006).

[15] K. Langanke, J.A. Maruhn and S. E. Koonin, Computational Nuclear Physics 1, Springer-Verlag (1991).

[16] W. A. Richter and B. A. Brown, Phys. Rev., C67 (2003) 034317.

[17] I. Angeli, At. Data Nucl. Data Tab. 78 (2004) 185.

[18] M. Brack, C. Guet and H. B. Hakansson, Phys. Lett. 5 (1985) 36.

[19] H. Uberall "Electron Scattering From Complex Nuclei (part A)" Academic Press-New York and London (1971).

[20] Y.S. Shen and Z.Z. Ren, Phys. Rev., C54 (1996) 1158.

[21] I. C. Brock, Physik V: Nuclear and Particle Physic (2012) 135.

[22] A. Ozawa, T. Suzuki and I. Tanihata, Nucl. Phys. A693 (2001) 32.